SOME RESULTS OF INVESTIGATIONS INTO THE OPTICAL AND MICROPHYSICAL CHARACTERISTICS OF SMOKES

A.A. Isakov

Institute of Atmospheric Physics,
Russian Academy of Sciences, Moscow
Received August 12, 1998

The data of experiments on studying the smokes (one tentative experiment and two complex studies) carried out in 1986–1988 are analyzed. The inverse problem has been solved for about fifty smokes. From these data we have reconstructed the particle size distributions and estimated the real and imaginary components of the refractive index of the particulate matter. It is shown that for most smokes the main mode of particles (i.e. the mode governing the optical characteristics of a smoke in the visible spectral region) is well described, in the first approximation, by a narrow single-mode lognormal size distribution. The size distribution of smoke particles and the complex refractive index of the particulate matter are analyzed in relation to burned materials and regimes of burning. We have used quasi-continuous spectral scanning when recording optical characteristics of smokes. The use of this method enabled us to reveal anomalies in the spectral behavior of optical properties of some smokes in the red portion of the spectral range studied. The calculations made using the model of harmonic oscillator have shown that such anomalies can be explained by the presence of an absorption band in this spectral range.

INTRODUCTION

This paper analyzes the data obtained for smoke aerosols with the help of the polarization spectronephelometer (hereinafter, PSN) in three experiments: the tentative one conducted in 1986 and the two complex experiments conducted in 1986 and 1988 at the Zvenigorod station of the Institute of Atmospheric Physics of RAS. In the tentative experiment, quite typical smoke aerosols were studied, such as those in the engine exhausts, cigarette and campfire smokes, etc. The complex experiments were conducted within the framework of the "Nuclear Winter" program, and the types of smokes under study were defined by this problem. Some results have been published in Refs. 1 and 2. The classification of smokes on the basis of their optical characteristics was proposed in Ref. 3. All smokes were divided into three groups: weakly absorbing coarse-disperse smokes (the first group), weakly absorbing fine-disperse ones (the second group), and strongly absorbing smokes (the third group). Almost all pyrolysis (smoldering) smokes fall in the first group. The second group mainly includes smokes from burning woods, peat, etc. The third group involves smokes from burning oil and rubber ("black" or "sooting up" smokes). In the subsequent discussion, we will follow this classification.

The first experiments have been aimed at studying optical and microphysical characteristics of smokes and were conducted at the Institute of Atmospheric Optics a decade earlier.[9,10] The statement of the problem was certainly somewhat different than that in the "Nuclear Winter" program, but the main conclusions[10] on the optical characteristics of smokes agree well with the outlined scheme. The equipment, smoke chamber, burned mixtures, and regimes of burning are described in Refs. 3 and 4. Let us only briefly remind here the main points of the complex experiments. The smoke chamber had the volume of 60 m^3. A smoke from the furnace came to the chamber through a pipe of 10-cm diameter and about 2 m long. A pre-weighted sample of a matter was burned in the electric furnace equipped with the devices for monitoring and regulating the regime of burning. Materials were burned at a temperature of 900° with the volume being blown through with air. Pyrolysis has proceeded at a temperature about 600° without air blowing.[4] Once a mixture has burned, a smoke in the chamber was mixed with a fan and then allowed to stay for about one hour and a half. This means that in the experiment we have studied optical characteristics of "aged" smokes generated under rather strictly fixed conditions. In the tentative experiment, to the contrary (except for the pyrolysis in a smoldering mode), the burning conditions – open fire, burning in

0235-6880/99/01 20-08 $02.00 © 1999 Institute of Atmospheric Optics

an engine cylinder – were different, and about 15 minutes passed from the time of burning to the termination of recording. In 1986, the spectronephelometer was set up near the smoke chamber, and a smoke was sucked in into the working chamber by its standard air sampler. In 1988, due to a radical modification of the device (see below), the spectronephelometer was set up in the laboratory, and a smoke was manually transported from the chamber to the device in a container with the volume about 10 liters.

A detailed description of the spectronephelometer can be found in Ref. 1. Let us remind the main performance characteristics of its version of 1986. The device measured the scattering phase function D_{11} at the scattering angles $\varphi = 45$ and 90°, as well as the degree of linear polarization of the scattered light at $\varphi = 90°$ at the four wavelengths $\lambda = 0.46$, 0.54, 0.68, and 0.8 μm. The spectral ranges were separated out with color-glass filters having half width about 15.0 nm. To study the extinction coefficient of smoke aerosols ξ, the device was specifically equipped with a 2-m long extension pipe, aligned coaxial with the light beam coming from the illuminator. The photoreceiver was set at its end to record the intensity of the beam having passed through a smoke. Thus, for every smoke the set of 16 optical parameters was measured.

In the process of analysis of the experimental results of 1986, the necessity to study more closely the spectral dependence of the scattering phase function and the extinction coefficient has been understood.[2,4,5] This study has been found to be urgent, because the spectral behavior of the extinction and scattering characteristics was obviously non-monotonic for the majority of smokes. In this connection, a new, in principle, illuminator has been built based on a SF16 monochromator. The spectral range of operation in the new modification of the nephelometer is $\lambda = 0.37$–0.85 μm when studying smoke aerosols, its spectral resolution (variable in the range, because the monochromator is a prism-based device) was 5.0–30.0 nm. For about half of all the smokes, the components of the scattering phase matrix were measured at a discrete set of wavelengths (20 points). For others, we used a computer to conduct the spectral scanning and recording.

In Ref. 1 the so-called "library" method was used to estimate the microphysical parameters of smoke aerosols. Following this method, the optical characteristics of scattering, which are most sensitive to variations of the particle size-distribution parameters, were revealed using model calculations. Then the nomogram grids were constructed, using which the microphysical parameters of smokes were estimated. The presence of absorption bands certainly was not analyzed in such a consideration. A more general statement of the inverse problem implies solution, in that or other way, of the integral equation relating the optical (components of the scattering phase matrix D) and microphysical parameters of smokes. Such a solution seemed to be too complicated for well known reasons: the kernel K of the equation to be solved contained the constants (i.e. the complex refractive index $m = n + i\chi$ of a particle matter), which should be determined along with the particle size-distribution function $N(r)$:

$$D(\varphi, \lambda) = \int K(\varphi, \lambda, m, r)\, N(r)\, \mathrm{d}r. \qquad (1)$$

Rapid development of computers has allowed changes in the approaches to solving similar inverse problems. It is not problematic nowadays to calculate a sufficient number of K values for Eq. (1) within the variation range of real component of the refractive index $n = 1.5 - 1.8$ and the imaginary component within the 0.0 – 0.2 range. The problem can be solved by a regularization method and by the exhaustive search among the K values for the smallest discrepancy. Certainly, such a technique cannot be considered as a general solution to the problem. At the same time, it is clear that the estimates of the refractive index and particle size-distribution obtained in such a way must be closer to real values than those obtained with the help of the "library" method.

Similar approach, based on the inversion of the polarization parameters (polarization components of the scattering phase function), is used in Ref. 9. It employs the same principle of minimum discrepancy to determine the optical constants of the particulate matter. The results of inversion of the smoke optical characteristics presented in Ref. 9 (the characteristic size of particles and the refractive index) well agree with the data we have obtained for similar smokes.

Analysis of the results of 1986 experiments has shown that some smokes have anomalous spectral dependence of the scattering phase function in the UV spectral range. The drastic decrease of D_{11} with the decreasing radiation wavelength is observed, what disagrees with the behavior of D_{11} in the visible spectral region. In Ref. 2, the anomalies are explained by the existence of two fractions in these smokes: a strongly absorbing fine-disperse fraction and a weakly absorbing coarse-disperse one. The fine-disperse fraction contributes insignificantly into the light scattering in the visible region. Its contribution is of the same order of magnitude as the measurement errors caused by fluctuations in smokes ($\approx 10\%$). Therefore, the data of the spectropolarimetry bear the information about the latter fraction only.

For some smokes, we also have detected non-monotonic spectral behavior in the red portion of the spectral range (the third filter of the PSN). Such a behavior is indicative of possible existence of an absorption band. The above-said has initiated the modification of the device. The detailed record of light scattering characteristics in the spectral range $\lambda = 0.6$–0.75 μm has really allowed us to detect simultaneous changes in the spectral behavior of the linear polarization of the scattered light and the

extinction coefficient ξ in the range $\lambda = 0.61–0.65$ μm for some smokes (see below). Note that the absorption band belonging to the carbon–nitrogen q–N-bond lies just in this range.

So, the problem of uncertain refractive index of a nucleus becomes more complicated due to possibly non-monotonic spectral behavior of n and χ. The problem stated in such a manner is obviously insoluble. Therefore, we use here the following scheme: since there are no reasonable grounds to believe that particles of the main (from the optical viewpoint) fraction have different chemical composition, nuclei are considered as having the constant refractive index over the entire spectral range, and possible anomalies are considered separately.

This method for estimation of microphysical parameters of smoke aerosols was applied in this work. The sensitivity of different optical characteristics to variations of optical constants of the particulate matter was previously estimated using the model of narrow lognormal distributions. These estimates have shown that for the above-mentioned 10% measurement error, the resolution limit for the real component of the refractive index is $\delta n \approx 0.05$, and for the imaginary component it is $\chi \approx 0.03$. "y the way, we have found that, for particles with radius $r \approx 0.3$ μm, introduction of even weak absorption $\chi = 0.03$ changes the normalized scattering phase function by about 1.5 times. Consequently, first, the main parameters for determination of the refractive index of absorbing smokes are the extinction coefficient ξ and the scattering phase function at the angle of 45°. More exactly, such a parameter is their ratio $K(\xi, D)$ or the normalized scattering phase function. Second, the optical response of a particle, along with the equivalent size following from a photoelectric counter data, changes correspondingly by 20–30%. Therefore, the results obtained in the complex experiments with the use of photoelectric counters should be considered critically, especially as concerning the absorbing smokes.

The iteration technique used for solution of the algebraized equation (1) is described in Ref. 8. For weakly absorbing smokes, the grid consisted of 30 nuclei. The variability range of a particle radius $r = 0.01–2.0$ μm was separated by twenty separation points. The step for the real component of the refractive index was 0.05, and for the imaginary component it was 0.03. For strongly absorbing smokes, the variability range of a radius was extended to $r = 3$ μm, and the range for the imaginary component of the refractive index was extended to $\chi = 0.4$.

THE RESULTS OF INVERSION OF THE SMOKE OPTICAL CHARACTERISTICS

Comparing the results of the two inversion methods, it is reasonable to make clear the following points: (1) how realistic are the results obtained with the use of the model single-mode lognormal distribution; (2) what additional information can be obtained with the use of the second method; (3) how completely do the above-mentioned 16 optical parameters describe the optics of smokes in the visible spectral region and how promising, from this point of view, is a more detailed spectral record; (4) how can possible spectral anomalies influence the solution of the inverse problem.

As was noted above, the steps in the real and imaginary components of the refractive index were in correspondence with their resolution (distinguishability) limit with the measurement error about 10%. This was confirmed by the results of solution of the inverse problem. The minimum discrepancies (usually differing by one percent and even smaller) were usually obtained for two neighboring values of the real component n. For the neighboring values of the imaginary component such values of the discrepancies occurred far more rarely. The latter ones were observed for smokes, the presence of an absorbing component in which could be expected *a priori*. The ordinary value of the discrepancy was about 10%. The results given by the two inversion methods are presented in the Table I, which compares the distribution parameters obtained in Refs. 1 and 2 for a dozen of smokes with the parameters of lognormal distribution optimally approximating the main distribution bell obtained for the same smokes from solution of the integral equation. The inverse problem was solved for about 50 different smokes.

The results of its solution demonstrate basically that the estimates made in Ref. 1 for a number of smokes (primarily for pyrolysis) proved to be a good approximation. The reconstructed distributions are well approximated by the model ones for about 70–80% of cases.

In the complex experiments, the conditions of smoke sampling were different. "esides, the tentative experiment and the complex differed in the conditions of burning. When compiling figures, we tried to underline manifestation of these factors in the formation of the microphysical characteristics of smoke aerosols. Since the distributions $dV(r)/dr$ of the pyrolysis smokes turned out to be similar in all the three experiments, there was no need to plot a separate figure for them. In our opinion, it is more important to compare them with other regimes of burning. The results of inversion are presented in Fig. 1 as particle size distributions. The smokes studied in the tentative experiment are shown in Figs. 1*a*, and *f*, and the smokes studied in the two complex experiments are shown in Figs. 1*b–e*. In Figs. 1*b*, *c*, and *e*, the $dV(r)/r$ curves for the smokes of diesel engine exhaust, peat and firewood burning are shown along with the lognormal distribution, to which they were fit. One circumstance engages our attention, because it possibly reflects the regularity in the processes of formation of smoke aerosols: if the left-hand wing of the distribution (corresponding to a smaller size) is usually well described by the model, then for the right-hand

wing it is the exception rather than the rule. In the latter case, either the distribution widens markedly as compared to the model one or the second fraction of particles becomes clearly seen in the size range $r \approx 0.8 - 1$ μm (Figs. 1 *a–c*). In Fig. 1*a*, where some weakly absorbing smokes of the tentative experiment are presented (wood pyrolysis smoke, engine exhaust, cigarette smoke), both types of deviations from the model distribution are clearly seen in the smoke of an idling diesel engine, and only widening of the right-hand wing is seen for the cigarette smoke. "y the way, the main distribution modes of these two smokes are surprisingly similar in both size and shape.

TABLE I.

Smoke source	Distribution parameters (the first method)				Parameters of the approximating distribution (the second method)			
	r	ν^2	n	χ	r	ν^2	n	χ
Tentative experiment								
Gasoline engine	0.03	0.5	1.55	0.1	0.1	0.1	1.5	0.0
Diesel engine, idling	0.11	0.2	1.5	0.0	0.13	0.15	1.55	0.0
Diesel engine, afterburner	0.27	0.1	1.54	0.2	0.23	0.1	1.65	0.2
Rubber, sooting-up flame	< 0.07	0.5	1.7	–	0.075	0.15	1.65	0.3
Organic glass, sooting-up flame	< 0.03	0.5	1.7	–	0.08	0.15	1.7	0.2
Spruce firewood	0.21	0.1	1.66	0.0	0.25	0.07	1.5	0.03
Pine firewood	0.19	0.1	1.66	0.0	0.25	0.07	1.5	0.03
Complex experiment of 1986								
Peat, burning No. 18	0.23	0.3	1.7	0.14	0.2	0.2	1.7	0.09
Peat, pyrolysis No. 17	0.25	0.3	1.68	0.05	0.22	0.2	1.7	0.03
Urban mixture, burning No. 4	0.28	0.3	1.68	0.05	0.28	0.15	1.75	0.03
Firewood mixture, burning No. 11	0.27	0.3	1.62	0.0	0.24	0.12	1.7	0.0
Firewood mixture, pyrolysis No. 12	0.24	0.3	1.56	0.05	0.16	0.3	1.7	0.06
Urban mixture, burning No. 16	0.25	0.3	1.7	0.1	0.27	0.07	1.7	0.09

In the visible spectral region, the optics of most smokes studied in the complex experiment is described by the optics of a narrow single-mode size distribution accurate to ≈10%. The values of the characteristic size of the most coarse-disperse smokes found by both methods are in a close correspondence. However, for many cases the method from Ref. 2 gives markedly more narrow distributions with the equivalent half width of the lognormal distribution up to $\nu^2 \approx 0.08$. The stable position of the distribution mode at the axis of particle radii and narrowness of the distribution suggest that there exists a mechanism, which is almost independent of a burned material. This mechanism strictly stabilizes the size distribution near a certain size of particles during the burning process. For the process of pyrolysis, such a size is $r = 0.25–0.3$ μm. The results of the complex and tentative experiments fall within this range. The burning mode for open flame and engine exhausts gives similar curves of narrow ($\nu^2 = 0.1$) distributions with $r = 0.08–0.1$ μm. In the complex experiments, burning proceeded at the oxygen deficit, and the burning smokes were more similar to pyrolysis smokes, rather than to open-flame smokes. This fact is embodied in the character of size distribution of their particles. The distribution width for them proved to be more strongly varying: $\nu^2 = 0.07–0.3$. For peat, for example, both modes have given very close distributions (see Fig. 1*b*). However, smoke particles generated in the pyrolysis mode were weakly absorbing $\chi \approx 0.03$, while those generated in the burning mode were strongly absorbing $\chi \approx 0.09$. Figure 1*c* illustrates how different (in microphysical characteristics) may be smokes originating from the same combustible material. The size distributions for particles of the two coal smokes studied in the experiments of 1986 (curve *1*) and 1988 (curve *2*, quasi-continuous scanning) are also presented here. The modal size in the latter smoke is three times larger than in the former one. An unusual distribution was observed for the wood smoke, when the firewood mixture included birch bark (Fig. 1*e*). It is the only smoke having the maximum of the particle size distribution at $r = 0.16$ μm. In other smokes, in the presence of the second mode of small particles (see Fig. 1*d*), a deep minimum always lies in this range, which separates the modes. In the tentative experiment,[1] the smoke originating from pure birch firewood was relatively fine-disperse and strongly absorbing ($r = 0.08$, $\chi \approx 0.1$). Therefore, we believe that the presence of bark in the sample has caused the character of the distribution.

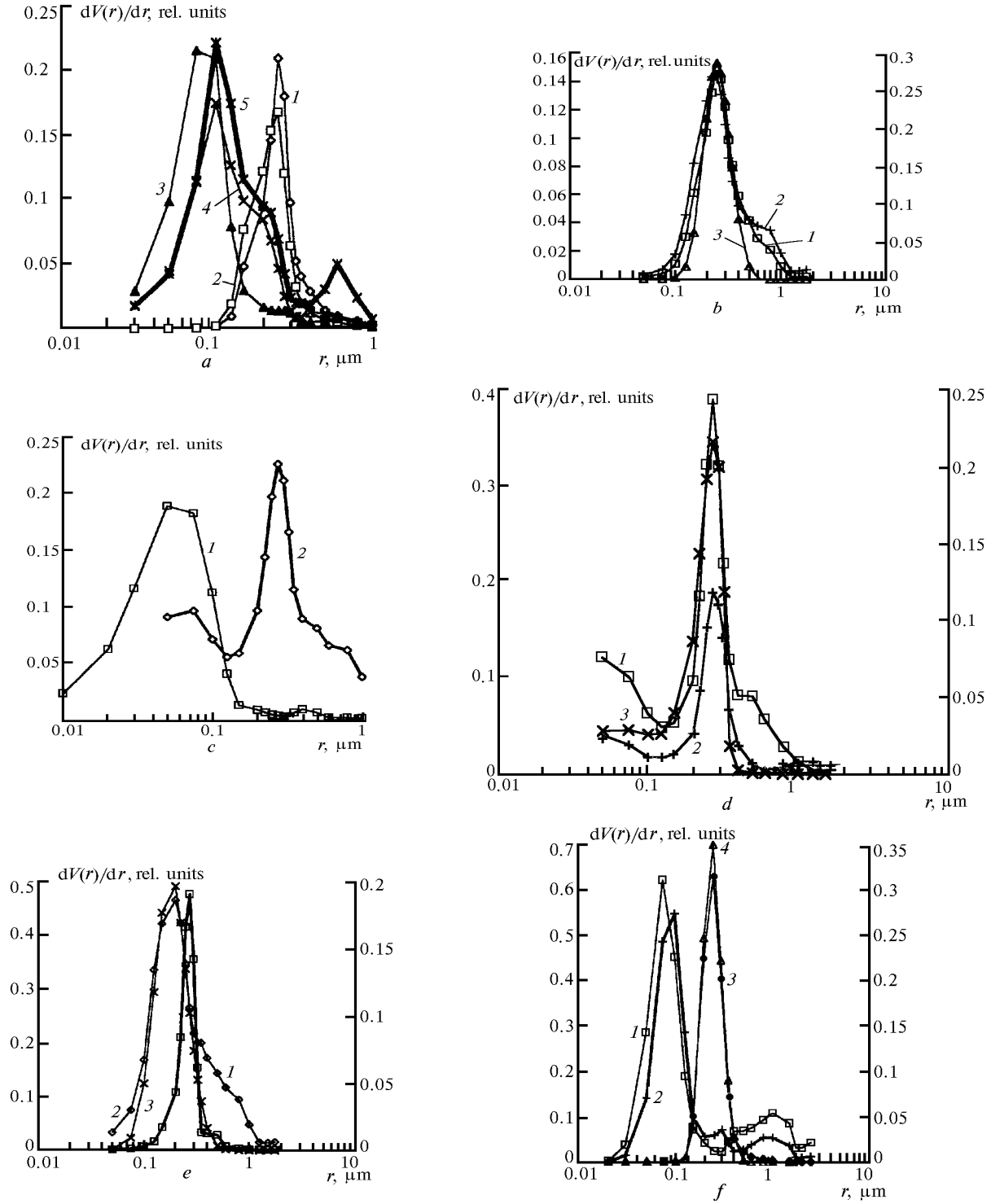

FIG. 1. Examples of reconstructed particle size-distributions $dV(r)/dr$: *(a) the tentative experiment: pine firewood, pyrolysis (curve 1), spruce firewood, pyrolysis (curve 2), gasoline engine exhaust (curve 3), cigarette smoke (curve 4), and exhaust of idling diesel engine (curve 5); (b) peat burning (curve 1) and pyrolysis (curve 2) smokes, the model distribution (curve 3); (c) coal smokes of 1986 (curve 1) and 1988 (curve 2); (d) the complex experiment of 1988: "urban mixture,B burning (curve 1), "urban mixture,B pyrolysis (curve 2), and firewood mixture, pyrolysis (curve 3); (e) "urban mixture,B pyrolysis (curve 1), firewood mixture with birch bark (curve 2), model distribution (curve 3); (f) "blackB smokes of the tentative experiment: organic glass (curve 1), rubber (curve 2), exhaust of a diesel engine in the afterburner mode (curve 3), model distribution (curve 4).*

Particular emphasis should be given to strongly absorbing "black" smokes. In Ref. 6, it was found, using the electrooptical instrumentation, that optical manifestation of the particle nonsphericity is completely absent only in pyrolysis smokes. In burning smokes, nonsphericity can manifest itself. It is especially true for "black" smokes. This effect is in a markedly large, about 15%, errors of reconstruction, what should be taken into account when considering Fig. 1*f*. As seen, the distribution in this case has, along with the main mode with the maximum at $r \approx 0.08$, the second wide maximum the near 1 μm. To study this size region of the particle size-distribution more thoroughly, we have calculated the grid with larger limit value of a radius and higher absorption, specifically for strongly absorbing smokes. Since the lifetime of these smokes is about 10 min, we can assume that the second maximum in the distribution corresponds to aggregates of soot particles, which do not yet sediment.

The exhaust of a diesel engine operating in the afterburner mode gave the only recorded smoke, for which the size distribution (see Fig. 1*e*) is similar to that for pyrolysis smoke, and the absorption factor $\chi \approx 0.2$ more likely corresponds to sooting-up fine-disperse smokes. "oth these methods give close estimates for its parameters and the parameters of an idling engine exhaust.

In the experiment of 1988, at its first stage, the scattering phase matrix was recorded at 20 wavelengths in the range of 0.37–0.85 μm. Changes in the spectral dependence of the degree of linear polarization were clearly seen for most smokes in the blue–violet spectral range (see the next section). So, to solve the inverse problem, we used the spectral range $\lambda = 0.45$–0.85. "esides, to reduce the number of reference points to seven (the step in wavelength $\Delta\lambda = 0.5$ μm), the approximating polynomials were constructed for all optical characteristics using the method of least squares. Note that, from the viewpoint of solution of the inverse problem, the detailed spectral record did not give a significant gain in information. This means that the sets of four wavelengths of twenty do not differ so much to change significantly the inverse problem solution. The distributions (see Fig. 1*d*) correspond to smokes studied in 1988. The only feature, which distinguishes them from other smokes, is the presence of the second mode of small particles. This means that sixteen parameters are quite sufficient for determination of at least the main mode.

Nevertheless, the detailed record is useful. First, the solution is most stable, when the number of measured parameters is equal or only a little more than the number of points at the distribution to be obtained. Second, it is just the results of 1988 that have allowed us to reveal the presence of the fine-disperse fraction with $r \approx 0.07 - 0.08$ in the markedly greater number (in percentage terms) of smokes, including the pyrolysis smokes. Third, the relative modal size of smoke particles is $\rho = 2\pi r/\lambda \approx 4$, that corresponds (for the observed values of the refractive index) to the position near the first maximum of the curve of the efficiency factor (the Stratton curve). "ecause of this, the maximum appears in the spectral dependence of the extinction coefficient ξ and D_{11} (45°) in the visible spectral region, when the particle size-distribution is narrow enough. With a given distribution, the exact position of the maximum depends on the refractive index of the particulate matter (by the way, variations of the refractive index can explain, at least partially, the variability of the spectral behavior of extinction, which was discussed in Ref. 5). Thus, the detailed spectral record allows a more reliable determination of the refractive index to be performed.

ANOMALIES IN THE SPECTRAL BEHAVIOR OF THE OPTICAL CHARACTERISTICS

The influence of an absorption band upon the spectral behavior of the optical characteristics of smoke aerosols can be followed up semi-quantitatively (see, for example, Ref. 6) using the simplest model of a harmonic oscillator. The frequency (ω) dependence of the real ε_1 and imaginary ε_2 components of the complex refractive index near the resonance frequency ω_0 of the harmonic oscillator is described by the following expression:

$$\varepsilon_1 = 1 + \frac{N f \left(\omega_0^2 - \omega^2\right)}{\left(\omega_0^2 - \omega^2\right)^2 + \gamma^2 \omega^2};$$

$$\varepsilon_2 = \frac{N f \gamma \omega}{\left(\omega_0^2 - \omega^2\right)^2 + \gamma^2 \omega^2}, \qquad (2)$$

where γ is the halfwidth of the resonance curve; f is the so-called oscillator strength, and N is the number of oscillators in a unit volume. From Eqs. (1) and (2), the expressions for the real n and imaginary χ components of the complex refractive index can be easily found:

$$n = \sqrt{\frac{\sqrt{\varepsilon_1^2 + \varepsilon_2^2} + \varepsilon_1}{2}}; \qquad (3)$$

$$\chi = \sqrt{\frac{\sqrt{\varepsilon_1^2 + \varepsilon_2^2} - \varepsilon_1}{2}}.$$

The real and imaginary components of the refractive index obey the Kramers–Kronig relationships. Therefore, in spite of the simplicity, the model can describe, at least semi-empirically, the real behavior of the optical constants of the particulate matter. The more or less realistic pattern of their behavior can be obtained by fitting the parameters f and γ.

The influence of an absorption band on the spectral behavior of the optical characteristics was calculated for the model lognormal distributions with the parameters typical for most smokes under study: the modal radius $r = 0.2–0.3$ μm and the distribution halfwidth $\nu = 0.07–0.1$. The band center was chosen at $\lambda = 0.6$ μm, and the relative band halfwidth was $\gamma = 0.05–0.1$. An example of calculated results is presented in Fig. 2. It is seen from Fig. 2 that the optical characteristics of smokes are very sensitive to the presence of absorption bands, and the strongest variations are caused by a decrease in the refractive index n in the region of anomalous dispersion.

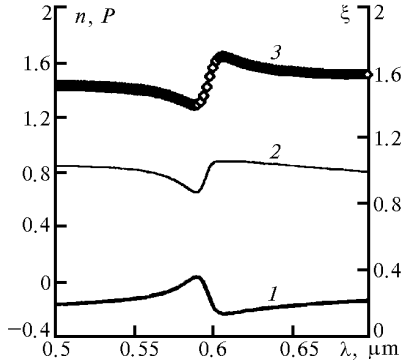

FIG. 2. The model of a harmonic oscillator; the spectral behavior near an absorption band: the degree of linear polarization of the scattered radiation p (curve 1), the real component of the refractive index n (the left-hand side ordinate), the extinction coefficient ξ (the right-hand side ordinate) for a lognormal particle size-distribution.

Figure 3 shows the spectral behavior of the same optical characteristics (the discrete set of wavelengths) obtained for the firewood smoke in the burning mode. As was noted above, signal fluctuations during the recording time were within 10%.

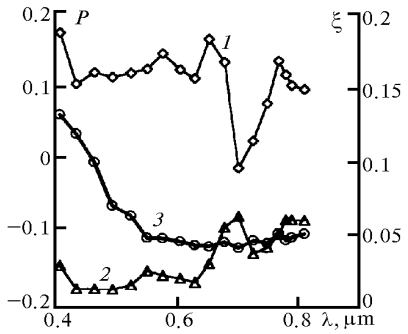

FIG. 3. The spectral behavior of the extinction coefficient (curve 1), the degree of linear polarization of the scattered light (curve 2) for the burning smoke of a firewood mixture, and the degree of polarization for the coal smoke (1988, quasi-continuous scanning) (curve 3).

The deep minimum far exceeding the total error was observed in the spectral behavior of the extinction coefficient near $\lambda \approx 0.65$ μm. It is just the range, where the maximum was observed in the spectral behavior of the degree of polarization, also significantly exceeding the total error. Similar but less pronounced behavior was observed for the pyrolysis smoke of the firewood mixture. The wavelength $\lambda = 0.61$ μm, at which this nonmonotonic behavior is observed, is shifted somewhat to the short-wave region.

The detailed spectral record has allowed a confirmation of the fast growth of the absorption (similarly to soot, "gray") in the blue–violet ($\lambda \le 0.45$ μm) spectral range for most smokes, in spite of possible presence of an absorption band in the red spectral region. Curve *3* in Fig. 3 (coal smoke) illustrates the alteration of the sign of polarization of scattered radiation in the violet spectral range, what is typical for many smokes. This clearly indicates towards the growth of absorption.

CONCLUSIONS

1. For most smokes, the optical characteristics in the visible spectral region are determined by the main fraction of particles, which is well described by a single-mode lognormal size distribution. Deviations from the model, if any, manifest themselves either in a significantly slower fall off of the distribution in the region of large sizes or in the second fraction of particles with the typical radius ~ 1 μm, sometimes as a fine-disperse mode of particle distribution that may appear at the particle radii $r < 0.1$ μm.

2. In the pyrolysis (smoldering) smokes, the particle size-distributions are narrow, with the halfwidth of the approximating lognormal distribution $\nu^2 = 0.07 - 0.15$ and the corresponding particle modal radius $r = 0.25 - 0.3$ μm, no matter what material was burned. The mechanism apparently exists which stabilizes the shape and size of particles. Absorption is practically absent in the visible region. The value of the refractive index depends on the material burned and varies within $n = 1.55 - 1.75$.

3. The particle size-distribution in the burning smokes depends significantly on the regime of burning. Open flame (and engine exhausts) produce fine-disperse particles with narrow size distributions (characteristic size $r = 0.07 - 0.1$). At the deficit of oxygen, even at the temperature of 900°q , the particle radii are close to those in pyrolysis smokes, and the size distribution is often wider $\nu^2 = 0.1 - 0.3$. Absorption may be zero (exhaust of a gasoline engine), weak ($\chi \approx 0.03$, wood of coniferous trees), medium ($\chi \approx 0.06$, birch bark, "urban mixture"), and strong ($\chi \approx 0.1 - 0.3$, sooting-up smokes of oil, organic glass, rubber, etc.). On average, the real component of the refractive index in the burning smokes is larger than that in the pyrolysis smokes. In the cases, when the fine-disperse and coarse-disperse fractions of particles

co-exist in a smoke, the minimum separating them practically always occurs at $r \approx 0.15$ μm.

4. In the visible spectral region $\lambda = 0.45 - 0.75$ μm (except for the anomalous sections), the optics of the main fraction is described, in the first approximation, by three to four components of the scattering phase matrix, measured at four wavelengths in this region. The ratio of the extinction coefficient to the parameter D (45°) is most significant for the determination of the imaginary component of the refractive index.

5. A detailed record of the spectral behavior of the smoke optical characteristics has allowed the detection of weakly selective absorption in the violet spectral range and, supposedly, an absorption band in the red spectral range for some smokes.

REFERENCES

1. V.V. Lukshin and A.A. Isakov, Izv. Akad. Nauk SSSR, Fiz. Atmos. Okeana **24**, No. 3, 250–257 (1988).
2. A.A. Isakov, V.V. Lukshin, and M.A. Sviridenkov, Izv. Akad. Nauk SSSR, Fiz. Atmos. Okeana **24**, No. 3, 258–262 (1988).
3. G.S. Golitsyn, A.Kh. Shukurov, A.S. Ginzburg, A.G. Sutugin, and A.V. Andronova, Izv. Akad. Nauk SSSR, Fiz. Atmos. Okeana **24**, No. 3, 227–234 (1988).
4. A.V. Andronova, E.M. Kostina, A.S. Kutov, V.M. Minashkin, S.M. Pirogov, Yu.I. Obvintsev, and A.G. Sutugin, Izv. Akad. Nauk SSSR, Fiz. Atmos. Okeana **24**, No. 3, 235–243 (1988).
5. P.P. Anikin and A.Kh. Shukurov, Izv. Akad. Nauk SSSR, Fiz. Atmos. Okeana **24**, No. 3, 244–249 (1988).
6. C.F. "ohren and D.R. Huffman, *Absorption and Scattering of Light by Small Particles* (Interscience–Wiley, New York, 1959).
7. V.H. Kapustin and A.A. Korneev, Izv. Akad. Nauk SSSR, Fiz. Atmos. Okeana **24**, No. 3, 280–289 (1988).
8. A.A. Isakov, Izv. Akad. Nauk SSSR, Fiz. Atmos. Okeana **30**, No. 2, 241–246 (1994).
9. V.V. Veretennikov, V.S. Kozlov, I.E. Naats, and V.Ya. Fadeev, Izv. Akad. Nauk SSSR, Fiz. Atmos. Okeana **16**, No. 3, 270–275 (1980).
10. Kozlov, M.V. Panchenko, and A.G. Tumakov, Atmos. Oceanic Opt. **6**, No. 10, 733–738 (1993).